



HAL
open science

Reactivity of dirhenium and triruthenium carbonyls toward a biphosphole ligand: M–M, P–P and C–H bonds cleavage

Yomaira Otero, David Coll, Alejandro Arce, Deisy Peña, Franmerly Fuentes, Muriel Hissler, Regis Réau, Rubén Machado, Teresa Gonzalez, Edward Ávila

► **To cite this version:**

Yomaira Otero, David Coll, Alejandro Arce, Deisy Peña, Franmerly Fuentes, et al.. Reactivity of dirhenium and triruthenium carbonyls toward a biphosphole ligand: M–M, P–P and C–H bonds cleavage. *Journal of Organometallic Chemistry*, 2017, 834, pp.40-46. 10.1016/j.jorganchem.2017.02.012 . hal-01468025

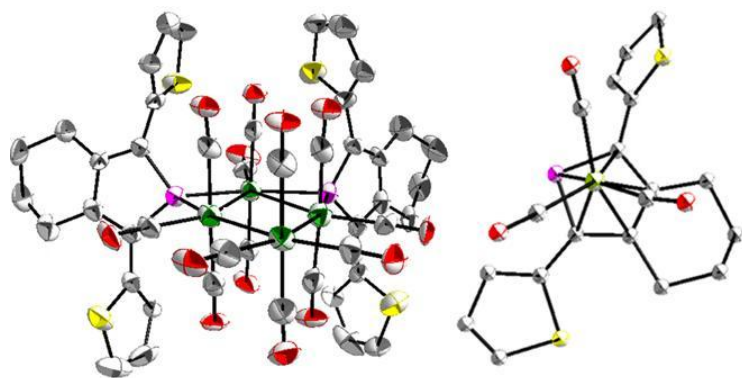
HAL Id: hal-01468025

<https://univ-rennes.hal.science/hal-01468025v1>

Submitted on 4 Jul 2017

HAL is a multi-disciplinary open access archive for the deposit and dissemination of scientific research documents, whether they are published or not. The documents may come from teaching and research institutions in France or abroad, or from public or private research centers.

L'archive ouverte pluridisciplinaire **HAL**, est destinée au dépôt et à la diffusion de documents scientifiques de niveau recherche, publiés ou non, émanant des établissements d'enseignement et de recherche français ou étrangers, des laboratoires publics ou privés.



1 **Reactivity of dirhenium and triruthenium carbonyls toward a biphosphole ligand:**

2 **M–M, P–P and C–H bonds cleavage**

3 Yomaira Otero^a, David Coll^{a,b}, Alejandro Arce^{a*}, Deisy Peña^a, Franmerly Fuentes^a, Muriel
4 Hissler^{c*}, Regis Réau^c, Rubén Machado^a, Teresa Gonzalez^a, Edward Ávila^a.

5 ^a*Centro de Química, Instituto Venezolano de Investigaciones Científicas (IVIC), Apartado 21827, Caracas 1020-A,*
6 *Venezuela.*

7 ^b*Escuela Superior Politécnica del Litoral, Centro de Investigación y Desarrollo de Nanotecnología, Ecuador.*

8 ^c*Institut des Sciences Chimiques de Rennes, UMR 6226, Université de Rennes 1, 35042 Rennes Cedex, France.*

9
10 *Corresponding authors:

11 Telephone number: +58 212 504 1322. e-mail address: aarce@ivic.gob.ve

12 Telephone number: +33 2 23 23 57 83. e-mail address: muriel.hissler@univ-rennes1.fr

13
14 **Abstract**

15 The reaction of $[\text{Re}_2(\text{CO})_8(\text{CH}_3\text{CN})_2]$ with bis(2-thienyl)biphosphole in refluxing *n*-octane affords
16 the complex $[\text{Re}(\text{CO})_3(\eta^5\text{-PC}_{16}\text{H}_{14}\text{S}_2)]$ (**1**) where cleavage of the Re–Re and P–P bonds occurs; its
17 molecular structure confirms the formation of a rhenium mononuclear compound with a η^5 -
18 coordinated phospholyl unit and three carbonyl groups oriented in a tripod. On the other hand,
19 bis(2-thienyl)biphosphole reacts with $[\text{Ru}_3(\text{CO})_{12}]$ in refluxing cyclohexane to affording two new
20 compounds $[\text{Ru}_3(\text{CO})_9(\mu:\eta^1:\eta^5\text{-PC}_{16}\text{H}_{13}\text{S}_2)]$ (**2**) and $[\text{Ru}_4(\text{CO})_{13}(\mu:\eta^1\text{-PC}_{16}\text{H}_{14}\text{S}_2)_2]$ (**3**).
21 Spectroscopic data and theoretical studies of **2** suggest the formation of an open Ru₃ cluster with
22 two metal–metal bonds bridged by a $(\eta^1:\eta^5\text{-PC}_{16}\text{H}_{13}\text{S}_2)$ unit and a C–H bond activation of one of the
23 thienyl substituents. X-ray structure of **3** reveals a novel tetranuclear ruthenium cluster containing
24 13 terminal carbonyl ligands and two phospholyl units coordinated as μ -phosphide.

25

26 **Keywords:** *Biphosphole; metal-metal and phosphorus-phosphorus bonds cleavage; tetranuclear*
27 *cluster; η^5 -phospholyl complex; C-H activation.*

28

29 **1. Introduction**

30 Heterocyclic π -complexes have been demonstrated to be excellent ligands for asymmetric catalysis
31 [1-5]. Particularly, phosphole ligands have been interesting for the development of complexes with
32 specific applications since they have the ability to act as both σ - and π -donor ligands, sometimes
33 simultaneously (Figure 1). Several phosphole-complexes have been used in catalytic
34 transformations, such as hydroformylation, hydrosilylation or asymmetric allylic substitution [6-9].
35 They have also been investigated in fields as diverse as OLEDs, WOLEDs and non linear optics
36 [10-12]. Additionally, phospholyl anions (phospholides) obtained from phosphole derivatives have
37 unique electronic properties since they are good π -acceptors and poor σ -donors [13-16]. They are
38 capable of η^1 - and η^5 -coordinating to metal centers (Figure 1) [17]. Particularly, η^5 -phospholyl
39 complexes have been used in numerous catalytic [4, 13, 14, 18-20].

40 On the other hand, organometallic compounds that incorporate two or more metal sites in close
41 proximity provide access to reaction pathways not available in mononuclear chemistry [21]. This
42 has been manifested, for example, in reversible metal–metal bond cleavage [22, 23], skeletal
43 rearrangement without degradation [24-26] and ligand activation via multisite coordination [27, 28].

44

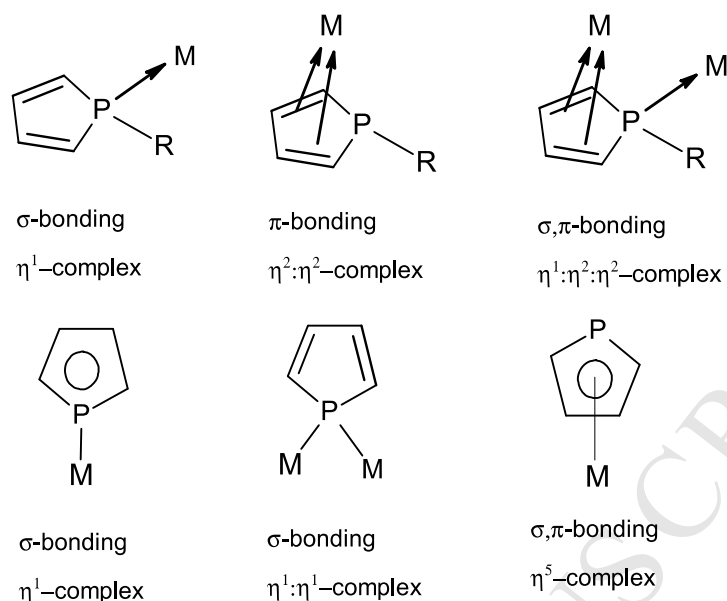


Figure 1. Coordination modes of phosphole and phospholyl ligands

45

46

47

48 In this regard, our studies have been focused on the reactivity of phosphorus derivatives, such as
 49 phosphines and phospholes, toward two or more metal centers, and we have found σ,π -complexes,
 50 derivatives containing ring-opened ligands, insertion of a phospholide unit into a metal–metal bond
 51 and bridging phosphide ligands [27, 29, 30]. Recently, we have studied the reaction of a variety of
 52 π -conjugated phosphole ligands with $[\text{Os}_3(\mu\text{-H})_2(\text{CO})_{10}]$ finding that the binding mode is restricted
 53 to σ -coordination, where electronic properties and steric effects of these phosphole ligands play a
 54 role in controlling the final product distribution and giving rise to a variety of isomers [31]. We are
 55 convinced that the coordination chemistry of phospholes is still a fertile area for further research.
 56 Thus, we have extended the study to the coordination chemistry of biphosphole derivatives on
 57 direnium and triruthenium carbonyls.

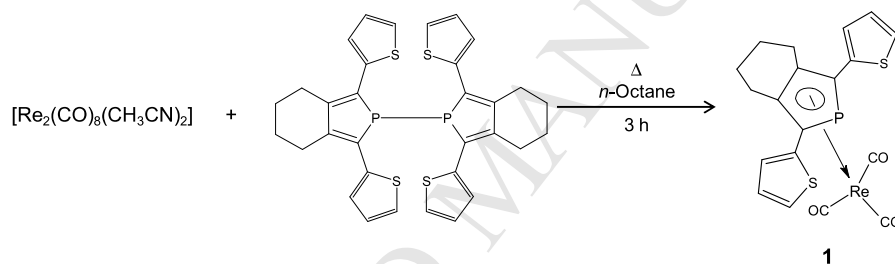
58

59

60

61 **2. Results and discussion**62 *2.1. Thermal treatment of [Re₂(CO)₈(CH₃CN)₂] with 2,2'-5,5'-tetra(2-thienyl)-1,1'-biphosphole*

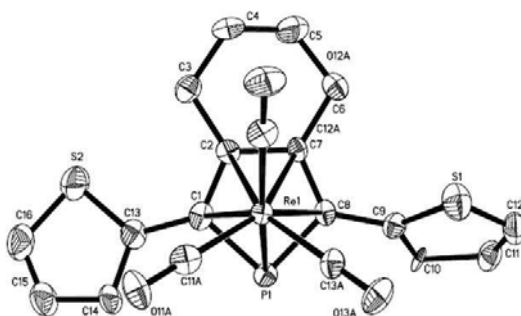
63 The reaction of [Re₂(CO)₈(CH₃CN)₂] with biphosphole ligand in refluxing *n*-octane affords one
 64 main compound characterized as [Re(CO)₃(η⁵-PC₁₆H₁₄S₂)] (**1**), (Scheme 1). Its ³¹P{¹H} NMR
 65 spectrum exhibits a singlet at δ -23.2, which is shifted upfield in comparison to the signal of free
 66 ligand (δ -0.1) [32], suggesting that the phosphorus atom is involved in the coordination to the
 67 metal center. The ¹H NMR spectrum does not show significant differences compared to those of the
 68 free ligand. However, in the ¹³C{¹H} NMR spectrum, signals for the dienic system are notably
 69 upfield shifted, indicating that coordination to the metal center by the dienic system has occurred.



70
 71 **Scheme 1.** Reaction of [Re₂(CO)₈(CH₃CN)₂] with bis(2-thienyl)biphosphole

72
 73 The molecular structure of compound **1** was determined by single crystal X-ray diffraction studies
 74 (See Figure 2, Table 1), which reveals a (η⁵-phospholy)rhenium complex obtained by cleavage of
 75 the Re–Re and P–P bonds of the starting materials. The complex is a rhenium mononuclear with
 76 three carbonyl groups in a tripodal orientation and one η⁵-PC₁₆H₁₄S₂ unit, molecular species with
 77 three-legged piano-stool geometry. The PC₁₆H₁₄S₂ moiety is coordinated as a phospholide to the
 78 rhenium atom [Re1–C1 = 2.36 (1) Å, Re1–C2 = 2.327(8) Å, Re1–C7 = 2.347 (7)Å, Re1–C8 =
 79 2.337 (7) Å, Re1–P1 = 2.530 (3) Å], resulting in a η⁵-complex. Phospholyl ring can be considered
 80 planar due to that the phosphorus atom lies 0.073 Å out of the mean plane containing the dienic
 81 moiety, and the bond delocalization is evidenced by the small deviation in inter atom distances

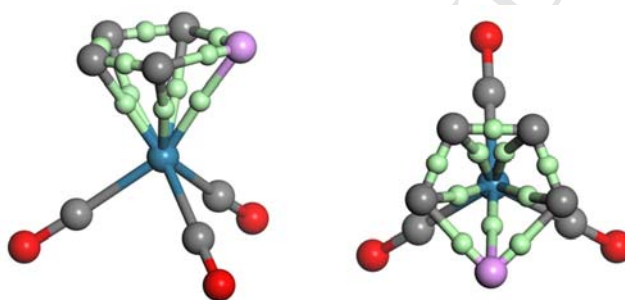
82 [C1–C2 = 1.45(1) Å, C2–C7 = 1.43(1) Å, C7–C8 = 1.42(1) Å, P1–C1 = 1.817(9) Å, P1–C8 =
 83 1.80(1) Å], similar to the reported for the analogous manganese derivative [Mn(CO)₃(η⁵-PC₉H₆)]
 84 [33].



85
 86 **Figure 2.** Molecular structure of **1**, showing 50% probability ellipsoids. Selected bond lengths (Å) and angles (°): Re1–
 87 P1 = 2.530 (3), Re1–C1 = 2.36 (1), Re1–C2 = 2.327 (8), Re1–C7 = 2.347 (7), Re1–C8 = 2.337 (7), P1–C1 = 1.817 (9),
 88 P1–C8 = 1.80 (1), C1–C2 = 1.45 (1), C2–C7 = 1.43 (1), C7–C8 = 1.42 (1), C11A–Re1–C12A = 91.5 (4), C11A–Re1–
 89 C13A = 90.3 (4), C12A–Re1–C13A = 90.7 (4).

90
 91 Additionally, the (η⁵-phospholyl)rhenium complex formation is corroborated by the presence of
 92 five bond critical points (BCP) between the rhenium atom and each element of the ring structure, as
 93 displayed in Figure 3. The electron density distribution of a free atom has spherical symmetry. Once
 94 this atom is bound, e.g. to form a molecule or a crystal, the electron density loses its spherical
 95 uniformity and this new distribution presents different types of critical points. The topological
 96 properties of a molecular or crystal charge distribution are summarized by its critical points (CP)
 97 [34]. These are points at which the gradient vector field, ∇F(r), vanishes. Among them there are
 98 maxima, minima and two types of saddle points. Every CP has a characteristic pattern of
 99 trajectories or gradient paths of F(r). The trajectories originate and end at critical points. For our
 100 purpose we are interested in two of them, the maxima CP which are associated to the nuclear
 101 positions, and one type of saddle points which is associated to the bond critical points (BCP). A
 102 BCP is found between every pair of neighboring nuclei. It represents both local maxima in two

103 directions and a local minimum in the third direction. The network of nuclei and BCP defines a
 104 graph, which describes the atomic connectivity and structure within a molecule or a crystal cell. In
 105 Figure 3, top and side views are presented for the molecular graph of the ring coordinated to the
 106 metal center, showing a “three legs stool” geometrical arrangement. For a better visualization, the
 107 rest of the elements in the structure are omitted. The magnitudes of the electron density over each
 108 BCP are similar, varying between 0.36 and 0.38 atomic units, which indicates that the electron
 109 density is consistently shared between the metal center and phospholyl ring. Theoretical
 110 calculations also indicate that the free energy of formation for compound **1**, based on the
 111 stoichiometrically balanced reaction, is +48 kcal/mol (Scheme 1).



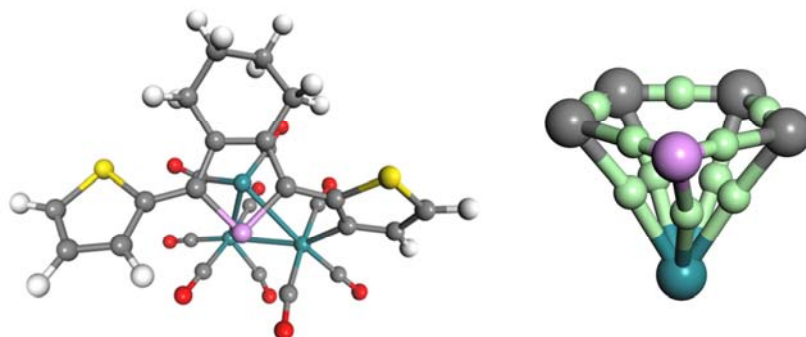
112
 113 **Figure 3.** Molecular graphs (top and side view) of the phosphorus ring coordinated to the metal center in **1**. Gray, red,
 114 blue and purple spheres represent C, O, Re and P atoms, respectively. Light green spheres represent the bond critical
 115 points (BCPs).

117 2.2 Thermal treatment of $[Ru_3(CO)_{12}]$ with 2,2'-5,5'-tetra(2-thienyl)-1,1'-biphosphole

118 Two new compounds were obtained by reaction of $[Ru_3(CO)_{12}]$ with 2,2'-5,5'-tetra(2-thienyl)-1,1'-
 119 biphosphole in refluxing cyclohexane, $[Ru_3(CO)_9(\mu:\eta^1:\eta^5-PC_{16}H_{13}S_2)]$ (**2**) and $[Ru_4(CO)_{13}(\mu:\eta^1-$
 120 $PC_{16}H_{14}S_2)_2]$ (**3**) (Scheme 2). The IR spectrum of compound **2** in the carbonyl region is
 121 characteristic of a nonacarbonyl trinuclear compound similar to $[Ru_3(CO)_9(\mu:\eta^1:\eta^5-PC_4H_2Me_2)(\eta^1-$
 122 $C_6H_5)]$ [27]. Its $^{31}P\{^1H\}$ NMR spectrum exhibits a singlet at δ 112.2, significantly downfield shifted

123 in comparison to the free ligand, similar to that observed for $[\text{Ru}_3(\text{CO})_9(\mu:\eta^1:\eta^5\text{-PC}_4\text{H}_2\text{Me}_2)(\eta^1\text{-}$
124 $\text{C}_6\text{H}_5)]$ [27]. The ^1H NMR spectrum of compound **2** shows two sets of signals for the thienyl
125 protons, showing inequivalence between both thienyl rings. Absence of the thienyl proton H_3 is also
126 observed, suggesting the occurrence of C-H bond activation. In the ^{13}C NMR spectrum, signals
127 assigned to the dienic system of the phosphorus ring are considerably upfieldshifted, similar to
128 those found for $[\text{Re}_2(\text{CO})_7(\mu:\eta^1:\eta^2:\eta^2\text{-PhPC}_4\text{H}_3\text{Me})]$, $[\text{Ru}_3(\text{CO})_9(\mu:\eta^1:\eta^5\text{-PC}_4\text{H}_2\text{Me}_2)(\eta^1\text{-C}_6\text{H}_5)]$ [27,
129 29, 30], indicating the coordination of the phospholyl ring to the trinuclear complex. The signal of
130 $\text{C}_{3\text{thienyl}}$ is downfield shifted, confirming the C-H bond activation. The ESI-MS spectrum of
131 compound **2** displays parent peaks of high intensity corresponding to its molecular ion $[\text{M}+\text{H}]^+$ at
132 m/z 858.79, which is in agreement with the molecular formula $[\text{Ru}_3(\text{CO})_9(\text{PC}_{16}\text{H}_{13}\text{S}_2)]$.
133 Unfortunately, we were unable to obtain suitable crystals of compound **2** for X-ray diffraction
134 analysis, however, based on the spectroscopic data and its comparison with the ruthenium analogue
135 $[\text{Ru}_3(\text{CO})_9(\mu:\eta^1:\eta^5\text{-PC}_4\text{H}_2\text{Me}_2)(\eta^1\text{-C}_6\text{H}_5)]$ [27], the proposed molecular structure of
136 $[\text{Ru}_3(\text{CO})_9(\mu:\eta^1:\eta^5\text{-PC}_{16}\text{H}_{13}\text{S}_2)]$ (**2**) is the most likely as shown in Scheme 2 . Thus, the structure
137 consists of an open Ru_3 cluster with two metal–metal bonds bridged by a $(\eta^1:\eta^5\text{-PC}_{16}\text{H}_{13}\text{S}_2)$ unit,
138 obtained probably by triple decarbonylation of $[\text{Ru}_3(\text{CO})_{12}]$, cleavage of a Ru–Ru and P–P bonds
139 and C–H activation of thienyl ring. Shift to higher values of the IR $\nu(\text{CO})$ frequencies as expected
140 for an anionic Ru_3 species was not observed for **2**, so an eight-electron donating ligand can be
141 considered in this case, which makes compound **2** a 50-electron cluster where each ruthenium atom
142 has the optimal 18-valence electron configuration.

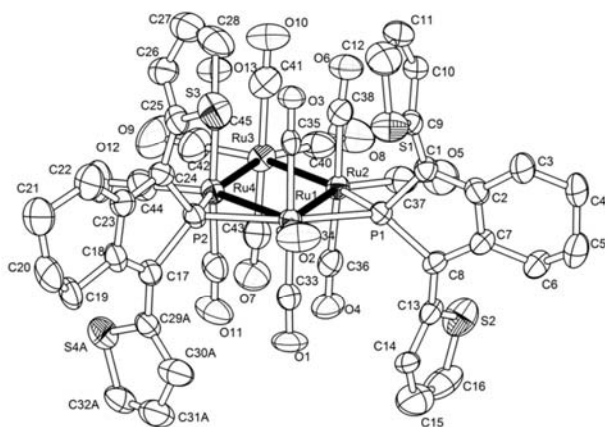
159 covalent interactions. The absence of a bond critical point between the two Ru atoms bound to two
 160 and three carbonyl ligands, respectively, indicates that the triruthenium structure is open.



161
 162 **Figure 4.** a) Most stable geometry for **2**. b) Molecular graph (side view) of the phosphorus ring coordinated to the metal
 163 center in **2**. Gray, red, blue, purple, white and yellow spheres represent C, O, Ru, P, H and S atoms, respectively. Light
 164 green spheres represent the bond critical points (BCPs).

165
 166 The ^{31}P , ^1H and ^{13}C NMR spectra of **3** suggest that a μ -phosphide coordination of the ligand is
 167 obtained; its molecular structure was determined by X-ray diffraction studies of crystals obtained by
 168 slow evaporation in a cyclohexane-dichloromethane mixture (See Figure 5, Table 1). The structure
 169 reveals a novel tetranuclear ruthenium cluster with 13 terminal carbonyl ligands and two phospholyl
 170 units, what are obtained from P-P bond cleavage in the biphosphole ligand. This makes each
 171 ruthenium atom have an effective atomic number equal to 54, according to EAN rule. The metal
 172 core can be described as a kite with four Ru–Ru bonds, two pairs of almost identical sides [Ru1–
 173 Ru2 = 3.137 (1) Å, Ru1–Ru4 = 3.136 (1) Å and Ru4–Ru3 = 2.930 (1), Ru2–Ru3 = 2.920 (1) Å]
 174 with angles two pairs similar [Ru2–Ru1–Ru4 = 60.16(2)°, Ru4–Ru3–Ru2 = 65.01(2)° and Ru1–
 175 Ru4–Ru3 = 117.25(2)°, Ru1–Ru2–Ru3 = 117.51(2)]. The axial carbonyl groups are eclipsed and
 176 both $\text{PC}_{16}\text{H}_{14}\text{S}_2$ moieties are coordinated as μ -phosphides. The two phosphorus atoms are nearly
 177 positioned in the same plane of the four ruthenium atoms [0.023 Å (P1) and 0.058 Å (P2)]. The
 178 Ru2–P1 [2.344(2) Å] and Ru4–P2 [2.340(2) Å] distances are slightly shorter than Ru1–P1 [2.396(2)

179 Å] and Ru1–P2 [2.387(2) Å], indicating that Ru1–Ru2 and Ru1–Ru4 edges are asymmetrically
 180 bridged by a phospholyl unit. The P1 and P2 atoms lie out of the plane of the diene system (0.094 Å
 181 and 0.022 Å respectively), describing the phosphorus rings with an opened envelope-type
 182 conformation.



183
 184 **Figure 5.** Molecular structure of **3**, showing 50% probability ellipsoids. Selected bond lengths (Å) and angles (°): Ru1–
 185 Ru2 = 3.137 (1), Ru1–Ru4 = 3.136 (1), Ru4–Ru3 = 2.930 (1), Ru2–Ru3 = 2.920 (1), Ru2–P1 = 2.344(2) Å, Ru4–P2 =
 186 2.340(2), Ru1–P1 = 2.396(2), Ru1–P2 = 2.387(2), Ru2–Ru1–Ru4 = 60.16(2), Ru4–Ru3–Ru2 = 65.01(2), Ru1–Ru4–Ru3
 187 = 117.25(2), Ru1–Ru2–Ru3 = 117.51(2).

188
 189 On the other hand, the molecular graph containing the metal core and its neighbouring atoms for
 190 compound **3** is shown in Figure 6. This graph displays two BCPs between each P atom and the two
 191 closest ruthenium atoms, corroborating the μ -phosphide coordination of the ligand. Interestingly,
 192 and in contrast to the X-ray molecular structure shown in Figure 5, Ru2 and Ru4 are bound while
 193 Ru1–Ru2 and Ru1–Ru4 bonds are not present, even though the observed internuclear Ru2–Ru4
 194 distance [3.144(1) Å] is longer than those for Ru1–Ru2 [3.137(1) Å] and Ru1–Ru4 [3.136(1) Å].
 195 As revealed in Figure 6, the BCP electron density value of Ru2–Ru4 bond is found to be smaller
 196 ($0.174 \text{ e}/\text{Å}^3$) than the ρ_{BCP} of Ru2–Ru3 and Ru3–Ru4 bonds (0.245 and $0.246 \text{ e}/\text{Å}^3$, respectively),
 197 indicating that no Ru2–Ru4 bond exists. This is consistent with the corresponding internuclear
 198 distances found with X-ray diffraction analyses.

199

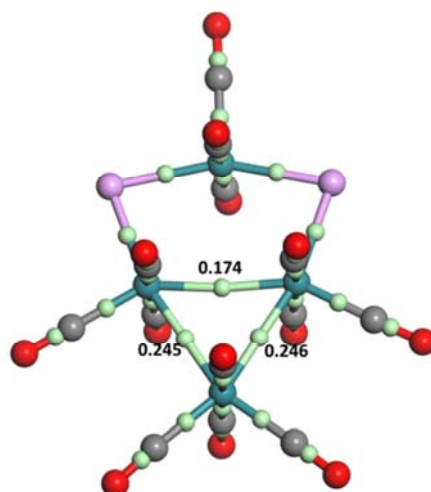


Figure 6. Molecular graph for the metal core of **3**. The BCP electron density values for Ru2–Ru4, Ru3–Ru4 and Ru2–Ru3 bonds are given in $e/\text{\AA}^3$. Bond distances are as presented in Table 1. Gray, red, blue and purple spheres represent C, O, Ru and P atoms, respectively. Light green spheres represent the bond critical points (BCPs).

3. Conclusions

A new (η^5 -phospholyl)rhenium complex $[\text{Re}(\text{CO})_3(\eta^5\text{-PC}_{16}\text{H}_{14}\text{S}_2)]$ (**1**) was obtained by the rhenium-rhenium and phosphorus-phosphorus bonds cleavage, when $[\text{Re}_2(\text{CO})_8(\text{CH}_3\text{CN})_2]$ reacts with bis(2-thienyl)biphosphole. Additionally, two new ruthenium carbonyl clusters were characterized as $[\text{Ru}_3(\text{CO})_9(\mu\text{-}\eta^1\text{-}\eta^5\text{-PC}_{16}\text{H}_{13}\text{S}_2)]$ (**2**) and $[\text{Ru}_4(\text{CO})_{13}(\mu\text{-}\eta^1\text{-PC}_{16}\text{H}_{14}\text{S}_2)_2]$ (**3**), wherein compound **2** represents the second example of a phospholide unit inserted into a metal–metal bond, while compound **3** is the first example of a tetranuclear cluster with two π -conjugated phospholyl units coordinated as μ -phosphides. These results open up the possibility for a facile access to new ruthenium and rhenium complexes with phospholyl units as bridging ligands which can be used in catalytic reactions.

4. Experimental section

4.1 General remarks

218 $[\text{Re}_2(\text{CO})_8(\text{CH}_3\text{CN})_2]$ and 2,2'-5,5'-tetra(2-thienyl)-1,1'-biphosphole were synthesized as
219 previously described [32, 35]. $[\text{Ru}_3(\text{CO})_{12}]$ was used as supplied by Aldrich Chemical Company.
220 ^1H , ^{13}C and ^{31}P NMR spectra were recorded using Bruker Avance AM300 and AM500
221 spectrometers, and assignment of carbon chemical shifts was based on HMBC and HMQC
222 experiment. Infrared spectra were recorded as cyclohexane solutions using a 2 mm CaF_2 cell on a
223 Spectrum 100 series Perkin Elmer spectrophotometer. Mass spectra were acquired on a Thermo
224 Scientific TSQ Quantum Ultra AM Triple Quadrupole mass spectrometer employing the Heated
225 Electrospray Ionization (HESI) technique. Routine separation of products in air was by thin-layer
226 chromatography on plates coated with Merck Kieselgel 60 GF₂₅₄.

228 4.2 Reaction of $[\text{Re}_2(\text{CO})_8(\text{CH}_3\text{CN})_2]$ with 2,2'-5,5'-tetra(2-thienyl)-1,1'-biphosphole

229 A solution of $[\text{Re}_2(\text{CO})_8(\text{CH}_3\text{CN})_2]$ (100 mg, 0.147 mmol) and 2,2'-5,5'-tetra(2-thienyl)-1,1'-
230 biphosphole (89 mg, 0.147 mmol) in dry *n*-octane (50mL) was taken to reflux under nitrogen for
231 3h. After evaporation of the solvent, TLC (SiO_2) of the brown solid residue
232 (hexane/dichloromethane, 9:1 v/v) gave $[\text{Re}(\text{CO})_3(\eta^5\text{-PC}_{16}\text{H}_{14}\text{S}_2)]$ (**1**) (89% yield). Spectral data for
233 **1**: IR (ν_{CO} , cyclohexane): 2026 (s), 1949 (s), 1935 (s) cm^{-1} . ^1H NMR (500 MHz, CD_2Cl_2): δ = 1.93
234 (m, 2H, $\text{CH}_2\text{-CH}_2\text{-C=C}$), 2.09 (m, 2H, $\text{CH}_2\text{-CH}_2\text{-C=C}$), 3.05 (m, 2H, $\text{CH}_2\text{-C=C}$), 3.17 (m, 2H, $\text{CH}_2\text{-C=C}$),
235 7.03 (d, $^4J_{\text{H}_5\text{-H}_3}$ = 1.6 Hz, 2H, H_3 thienyl), 7.04 (d, $^3J_{\text{H}_5\text{-H}_4}$ = 4.7 Hz, 2H, H_4 thienyl), 7.34 (dd,
236 $^3J_{\text{H}_4\text{-H}_5}$ = 4.7 Hz, $^4J_{\text{H}_3\text{-H}_5}$ = 1.6 Hz, 2H, H_5 thienyl). $^{13}\text{C}\{^1\text{H}\}$ NMR (500 MHz, CD_2Cl_2): δ = 22.6 (s,
237 $\text{CH}_2\text{-CH}_2\text{-C=C}$), 26.3 (s, $\text{CH}_2\text{-C=C}$), 109.1 (d, $J_{\text{P-C}}$ = 23.0 Hz, C_α), 114.6 (d, $^2J_{\text{P-C}}$ = 4.9 Hz, C_β),
238 126.6 (s, C_5 thienyl), 127.3 (s, C_4 thienyl), 128.5 (d, $^3J_{\text{P-C}}$ = 6.8 Hz, C_3 thienyl), 136.2 (d, $^2J_{\text{P-C}}$ = 20.3 Hz,
239 C_2 thienyl), 194.4 (s, M-CO). $^{31}\text{P}\{^1\text{H}\}$ NMR (500 MHz, CDCl_3): δ = -23.2 (s). MS: m/z 373.24
240 $[\text{M}+\text{H}]^+$.

241

242 4.3 Reaction of $[Ru_3(CO)_{12}]$ with 2,2'-5,5'-tetra(2-thienyl)-1,1'-biphosphole

243 A solution of $[Ru_3(CO)_{12}]$ (100 mg, 0.156 mmol) and 2,2'-5,5'-tetra(2-thienyl)-1,1'-biphosphole
 244 (94 mg, 0.156 mmol) in dry cyclohexane (50mL) was taken to reflux under nitrogen for 2h. After
 245 evaporation of the solvent, TLC (SiO_2) of the brown solid residue (hexane/dichloromethane, 8:2
 246 v/v) gave two compounds $[Ru_3(CO)_9(\mu.\eta^1:\eta^5-PC_{16}H_{13}S_2)]$ (**2**) (19% yield), and $[Ru_4(CO)_{13}(\mu.\eta^1-$
 247 $PC_{16}H_{13}S_2)_2]$ (**3**) (35% yield). Spectral data for **2**: IR (ν_{CO} , cyclohexane): 2109 (m), 2063 (s), 2048
 248 (s), 2026 (s), 2016 (m), 1999 (m), 1984 (w), 1949 (w) cm^{-1} . 1H NMR (300 MHz, CD_2Cl_2): δ = 2.16
 249 (m, 2H, $CH_2-CH_2-C=C$), 2.31 (m, 2H, $CH_2-CH_2-C=C$), 2.81 (m, 1H, $CH_2-C=C$), 3.08 (m, 2H,
 250 $^*CH_2-C=C$), 3.30 (m, 1H, $CH_2-C=C$), 6.82 (dd, $^3J_{H4-H5}$ = 4.8 Hz, $^3J_{H4-H3}$ = 3.6 Hz, 1H, H_4 thienyl),
 251 6.88 (dd, $^3J_{H3-H4}$ = 3.6 Hz, $^4J_{H3-H5}$ = 1.1 Hz, 1H, H_3 thienyl), 7.02 (d, $^3J_{H4^*-H5^*}$ = 4.9 Hz, 1H, H_{4^*} thienyl),
 252 7.17 (dd, $^3J_{H5-H4}$ = 4.8 Hz, $^4J_{H5-H3}$ = 1.8 Hz, 1H, H_5 thienyl), 7.25 (dd, $^3J_{H5^*-H4^*}$ = 4.9 Hz, $^5J_{H5^*-P}$ = 1.3
 253 Hz, 1H, H_{5^*} thienyl). $^{13}C\{^1H\}$ NMR (300 MHz, CD_2Cl_2): δ = 23.0 (s, $CH_2-CH_2-C=C$), 23.7 (s, $^*CH_2-$
 254 $CH_2-C=C$), 25.4 (d, $^2J_{P-C}$ = 5.3 Hz, $^*CH_2-C=C$), 26.2 (d, $^2J_{P-C}$ = 3.9 Hz, $CH_2-C=C$), 54.5 (s, C_{6^*}
 255 thienyl), 57.2 (s, C_6 thienyl), 98.6 (s, C_{7^*} thienyl), 98.9 (s, C_7 thienyl), 127.1 (s, C_{5^*} thienyl), 127.2 (s, C_5 thienyl),
 256 127.7 (s, C_4 thienyl), 130.0 (d, $^3J_{P-C}$ = 7.2 Hz, C_3 thienyl), 135.6 (s, C_2 thienyl) 135.8 (s, C_{2^*} thienyl), 137.4 (s,
 257 C_4 thienyl), 160.6 (s, C_{3^*} thienyl), 195.4 (s, M-CO), 203.2 (s, M-CO), 205.9 (s, M-CO). $^{31}P\{^1H\}$ NMR
 258 (500 MHz, CD_2Cl_2): δ = 112.2 (s). MS: 858.79 m/z $[M+H]^+$. Spectral data for **3**: IR (ν_{CO} ,
 259 cyclohexane): 2105 (w), 2079 (m), 2042 (s), 2015 (m), 1995 (m), 1975 (w) cm^{-1} . 1H NMR (500
 260 MHz, CD_2Cl_2): δ = 1.73 (m, 4H, $CH_2-CH_2-C=C$), 2.44 (m, 4H, $CH_2-C=C$), 6.90 (dd, $^4J_{H5-H3}$ = 1.0
 261 Hz, $^3J_{H4-H3}$ = 3.5 Hz, 2H, H_3 thienyl), 6.97 (dd, $^3J_{H5-H4}$ = 5.1 Hz, $^3J_{H3-H4}$ = 3.5 Hz, 2H, H_4 thienyl), 7.39
 262 (dd, $^3J_{H4-H5}$ = 5.1 Hz, $^4J_{H3-H5}$ = 1.0 Hz, 2H, H_5 thienyl). $^{13}C\{^1H\}$ NMR (500 MHz, CD_2Cl_2): δ = 22.8 (s,
 263 $CH_2-CH_2-C=C$), 28.4 (s, $CH_2-C=C$), 127.2 (s, C_4 thienyl), 127.6 (s, C_5 thienyl), 129.6 (s, C_3 thienyl), 136.4
 264 (s, C_2 thienyl), 139.2 (s, C_α), 150.3 (s, C_β), 206.2 (s, M-CO). $^{31}P\{^1H\}$ NMR (500 MHz, $CDCl_3$): δ =
 265 84.4 (s). MS: m/z 1371.00 $[M+H]^+$.

266

267 *4.4 Crystal structure determination for 1 and 3*

268 Intensity data were recorded at room temperature on a Rigaku AFC-7S diffractometer equipped
269 with a Mercury CCD detector using monochromated Mo(K α) radiation ($\lambda = 0.71070 \text{ \AA}$). An
270 empirical absorption correction (multi-scan) was applied using the CrystalClear package. The low
271 completeness ratio is due to the experimental setup whereby by the equipment have a ω circle and
272 an added area detector (four-circle diffractometer modified with a CCD). This precludes the
273 collection of some regions of reciprocal lattice space and lowers the completeness. In order to
274 compensate, additional redundant data were measured. The structures were solved by direct
275 methods and refined by full-matrix least-squares on F² using the SHELXTL-PLUS package. All
276 non hydrogen atoms were refined anisotropically, and hydrogen atoms were added at calculated
277 positions (C-H = 0.93–0.97 \AA) and refined as riding with $U_{\text{iso}}(\text{H}) = 1.2U_{\text{eq}}$. One crystallographically
278 independent dichloromethane molecule located on special positions was found disordered. Attempts
279 were made to model this disorder or split it into two positions, but were unsuccessful.
280 PLATON/SQUEZZE routine was used to correct the data for the presence of two disordered
281 solvent. A potential solvent volume of 461 \AA^3 was found. The stoichiometry of the solvent was
282 calculated to be 1 molecule of dichloromethane per formula unit, which results in a total of 125
283 electrons per unit cell. This molecule was used to calculate expected molecular weight, D_X calc and
284 $F(000)$. Additionally, we have managed to solve the disorder of the S4 atom with a thorough
285 revision of the map of Fourier differences, managing to model not only the disorder of the atom S4
286 but the complete thienyl group to which it belongs; C29-S4-C30-C31-C32 atoms, which group has
287 a 60.8% disorder. Therefore, considering this disorder we find that the bond distance for the C29-
288 C30 is 1.434 \AA , whose distance is inside the maximum (1.819 \AA) and minimum (1.053 \AA) values
289 and average of 1.343(36) \AA for similar structures in a search made with Mogul 1.7.1 build RC2.

290 Crystal and refinement information for compounds **1** and **3** is showed in Table 1. CCDC 1497908
 291 and 1497909 contain the supplementary crystallographic data for compounds **1** and **3**, respectively.
 292 These data can be obtained free of charge from The Cambridge Crystallographic Data Center via
 293 www.ccdc.cam.ac.uk/data_request/cif.

294
 295 **Table 1.** Experimental details for X-ray diffraction collected data and structural refinement for compounds **1** and **3**.

	[Re(CO)₃(η^5-PC₁₆H₁₄S₂)] (1)	[Ru₄(CO)₁₃(μ-PC₁₆H₁₃S₂)₂] (3)
Chemical formula	C ₁₉ H ₁₄ O ₃ PREs ₂	C _{46.5} H ₃₁ Cl ₃ O ₁₃ P ₂ Ru ₄ S ₄
Formula weight	571.59	1498.52
Crystal system, Space group	Triclinic, <i>P</i> -1 (No. 2)	Triclinic, <i>P</i> -1 (No. 2)
a(Å), α (°)	9.746(6), 98.363(9)	12.058(2), 74.21(3)
b(Å), β (°)	10.127(5), 111.609(15)	14.584(3), 71.28(2)
c(Å), γ (°)	10.340(6), 91.830(18)	17.487(3), 72.92(2)
V(Å ³), Z	934.7(9), 2	2729.8(11), 2
dx (g cm ⁻³)	2.031	1.823
Crystal size (mm)	0.05 × 0.14 × 0.16	0.44 × 0.40 × 0.36
F(000)	548	1470
μ (mm ⁻¹)	6.826	1.503
θ range (°)	2.0414 – 27.4333	1.254 – 27.573
Reflections Collected	10362	25543
Reflections Unique(R_{int})	3359	9350
Reflections With $I > 2\sigma(I)$	3084	7075
Number of parameters	235	629
R(F^2) [$I > 2\sigma(I)$]	0.046	0.050
wR(F^2) [$I > 2r(I)$]	0.120	0.155
Goodness of fit on F^2	1.07	1.10
Max/min $\Delta\rho$ (e Å ⁻³)	1.82 – 2.43	1.60 – 0.83

296

297 4.5 Theoretical calculations

298 All structures were optimized using DMol³ [36–38]. This DFT based program permits determination
 299 of the relative stability of all studied species based on their electronic structure. The calculations
 300 were performed using the Kohn–Sham Hamiltonian with the Perdew–Wang 1991 gradient
 301 correction [39] and the double-zeta plus (DNP) numerical basic set [36, 37, 40], which provides
 302 good accuracy at a relatively low computational cost. The All Electron core treatment was used for
 303 all the atoms. Frequency calculations of the structures showed that all frequencies were positive

304 indicating that all structures are real minima. The presence and nature of the chemical bonds, has
305 been analyzed using the quantum theory of atoms in molecules (QTAIM) [34] and the AIM-UC
306 code [41].

307

308 Acknowledgements

309 We thank FONACIT and Laboratorio Nacional de Difracción de Rayos-X for funding the projects
310 G-20050000447 and LAB-97000821, respectively. Additionally, we thank to the Programa de
311 Cooperación de Post-grado (PCP) between France and Venezuela.

312

313 References

- 314 [1] C. Ganter, The chemistry of chiral heterometalloenes, *J. Chem. Soc., Dalton Trans.* (24) (2001) 3541-3548.
315 [2] F.O. Mathey, Phosphorus-carbon heterocyclic chemistry : the rise of a new domain, Pergamon, Amsterdam; New
316 York, 2001.
317 [3] A.J. Ashe Iii, S. Al-Ahmad, Diheteroferrocenes and Related Derivatives of the Group 15 Elements: Arsenic,
318 Antimony, and Bismuth, in: A.S. F. Gordon, W. Robert (Eds.), *Adv. Organomet. Chem.*, Academic Press 1996, pp. 325-
319 353.
320 [4] F. Mathey, The chemistry of phospho- and polyphosphacyclopentadienide anions, *Coord. Chem. Rev.* 137 (1994) 1-
321 52.
322 [5] K.B. Dillon, Phosphorus : the carbon copy : from organophosphorus to phospho-organic chemistry, in: F. Mathey,
323 J.F. Nixon (Eds.) John Wiley, Chichester, England ;, 1998.
324 [6] G. Mora, B. Deschamps, S. van Zutphen, X.F. Le Goff, L. Ricard, P. Le Floch, Xanthene-Phosphole Ligands:
325 Synthesis, Coordination Chemistry, and Activity in the Palladium-Catalyzed Amine Allylation, *Organometallics* 26(8)
326 (2007) 1846-1855.
327 [7] S. Doherty, E.G. Robins, J.G. Knight, C.R. Newman, B. Rhodes, P.A. Champkin, W. Clegg, Selectivity for the
328 methoxycarbonylation of ethylene versus CO₂ ethylene copolymerization with catalysts based on C4-bridged bidentate
329 phosphines and phospholes, *J. Organomet. Chem.* 640(1-2) (2001) 182-196.
330 [8] J. Hydrio, M. Gouygou, F. Dallemer, J.-C. Daran, G.G.A. Balavoine, New chiral phosphole ligands: their
331 coordination behaviour and application in palladium-catalysed asymmetric allylic substitution, *Tetrahedron:*
332 *Asymmetry* 13(10) (2002) 1097-1102.
333 [9] G. Keglevich, T. Kégl, T. Chuluunbaatar, B. Dajka, P. Mátyus, B. Balogh, L. Kollár, Hydroformylation of styrene in
334 the presence of rhodium-2,4,6-trialkylphenyl-phosphole in situ catalytic systems, *J. Mol. Catal. A: Chem.* 200(1-2)
335 (2003) 131-136.
336 [10] P.-A. Bouit, A. Escande, R. Szűcs, D. Szieberth, C. Lescop, L. Nyulászi, M. Hissler, R. Réau,
337 Dibenzophosphapentaphenes: Exploiting P Chemistry for Gap Fine-Tuning and Coordination-Driven Assembly of
338 Planar Polycyclic Aromatic Hydrocarbons, *J. Am. Chem. Soc.* 134(15) (2012) 6524-6527.
339 [11] H. Chen, W. Delaunay, L. Yu, D. Joly, Z. Wang, J. Li, Z. Wang, C. Lescop, D. Tondelier, B. Geffroy, Z. Duan, M.
340 Hissler, F. Mathey, R. Réau, 2,2'-Biphospholes: Building Blocks for Tuning the HOMO-LUMO Gap of π -Systems
341 Using Covalent Bonding and Metal Coordination, *Angew. Chem. Int. Ed.* 51(1) (2012) 214-217.
342 [12] J. Crassous, R. Reau, [small pi]-Conjugated phosphole derivatives: synthesis, optoelectronic functions and
343 coordination chemistry, *Dalton Transactions* (48) (2008) 6865-6876.
344 [13] F. Mathey, Phosphametalloenes: from discovery to applications, *J. Organomet. Chem.* 646(1-2) (2002) 15-20.
345 [14] P.L. Floch, Phosphaalkene, phospholyl and phosphinine ligands: New tools in coordination chemistry and
346 catalysis, *Coord. Chem. Rev.* 250(5-6) (2006) 627-681.

- 347 [15] M. Ogasawara, S. Arae, S. Watanabe, V. Subbarayan, H. Sato, T. Takahashi, Synthesis and Characterization of
348 Benzo[b]phosphaferrocene Derivatives, *Organometallics* 32(17) (2013) 4997-5000.
- 349 [16] H.-C. Su, O. Fadhel, C.-J. Yang, T.-Y. Cho, C. Fave, M. Hissler, C.-C. Wu, R. Réau, Toward Functional π -
350 Conjugated Organophosphorus Materials: Design of Phosphole-Based Oligomers for Electroluminescent Devices, *J.*
351 *Am. Chem. Soc.* 128(3) (2006) 983-995.
- 352 [17] Y.J. Ahn, R.J. Rubio, T.K. Hollis, F.S. Tham, B. Donnadieu, Slip–Inversion–Slip Mechanism of
353 Phosphametalocene Isomerization. Spectroscopic Characterization of an (η 1-Phospholyl)titanium Complex. Synthesis
354 and Structures of Chiral Mono(phospholyl)titanium Complexes, *Organometallics* 25(5) (2006) 1079-1083.
- 355 [18] D. Carmichael, F. Mathey, L. Ricard, N. Seeboth, Synthesis of 2-silyl substituted phospharuthenocenes and an
356 elaboration into the first phospharuthenocene-phosphine, *Chem. Commun.* (24) (2002) 2976-2977.
- 357 [19] L. Weber, Phosphorus Heterocycles: From Laboratory Curiosities to Ligands in Highly Efficient Catalysts, *Angew.*
358 *Chem. Int. Ed.* 41(4) (2002) 563-572.
- 359 [20] F. Nief, F. Mathey, L. Ricard, F. Robert, Coordination chemistry of the new 2,3,4,5-tetramethylphospholyl
360 (C4Me4P) π -ligand. Crystal and molecular structure of $(\eta^5\text{-C}_4\text{Me}_4\text{P})_2\text{ZrCl}_2 \cdot 1/2\text{C}_{10}\text{H}_8$, *Organometallics*
361 7(4) (1988) 921-926.
- 362 [21] P. Braunstein, Workshop on Clusters and Surfaces Interplay between bridging groups and metal-metal bonds in
363 heterometallic clusters, *Mater. Chem. Phys.* 29(1) (1991) 33-63.
- 364 [22] G. Huttner, J. Schneider, H.-D. Müller, G. Mohr, J. von Seyerl, L. Wohlfahrt, Reversible Opening of a Trinuclear
365 Heterometal Cluster, *Angewandte Chemie International Edition in English* 18(1) (1979) 76-77.
- 366 [23] F. Richter, H. Vahrenkamp, Basic cluster reactions. 1. Reversible unfolding of FeCo₂Mo and FeCo₂W clusters,
367 *Organometallics* 1(5) (1982) 756-757.
- 368 [24] M.I. Bruce, J.G. Matison, J.R. Rodgers, R.C. Wallis, Cluster chemistry. Synthesis and X-ray structure of
369 [Ru₅(CO)₁₄(CNBut)₂], containing an unusual open Ru₅ cluster, *J. Chem. Soc., Chem. Commun.* (20) (1981) 1070-
370 1071.
- 371 [25] D.H. Farrar, P.F. Jackson, B.F.G. Johnson, J. Lewis, J.N. Nicholls, M. McPartlin, A high-yield synthesis of
372 Ru₅C(CO)₁₅ by the carbonylation of Ru₆C(CO)₁₇; the X-ray structure analyses of Ru₅C(CO)₁₅ and
373 Ru₅C(CO)₁₄PPPh₃, *J. Chem. Soc., Chem. Commun.* (9) (1981) 415-416.
- 374 [26] R.D. Adams, M. Chen, X. Yang, Iridium–Gold Cluster Compounds: Syntheses, Structures, and an Unusual
375 Ligand-Induced Skeletal Rearrangement, *Organometallics* 31(9) (2012) 3588-3598.
- 376 [27] A.J. Arce, Y. De Sanctis, M.C. Goite, R. Machado, Y. Otero, T. Gonzalez, Insertion of a phospholide unit into a
377 metal–metal bond: Synthesis and X-ray structure of [Ru₃(CO)₉(μ : η 1: η 5-PC₄H₂Me₂)(η 1-C₆H₅)], *Inorg. Chim. Acta*
378 392(0) (2012) 241-245.
- 379 [28] A.J. Arce, Y. De Sanctis, J. Manzur, A.J. Deeming, N.I. Powell, Oxidative addition of phenylphosphole: X-ray
380 crystal structures of two ring-opened products [Os₃(μ 3-PhPC₄H₄)(CO)_x] where x = 8 or 9, *J. Organomet. Chem.*
381 408(1) (1991) C18-C21.
- 382 [29] Y. Otero, A. Arce, Y.D. Sanctis, R. Machado, M.C. Goite, T. Gonzalez, A. Briceño, High versatility of 3,4-
383 dimethyl-1-phenyl-phosphole and 3-methyl-1-phenyl-phosphole as ligands in the reaction with [Re₂(CO)₈(CH₃CN)₂]
384 and [Ru₃(CO)₁₂]: X-ray structures of [Re₂(CO)₇(η 1: η 2: η 2-PhPC₄H₂Me₂)], [Re₂(CO)₇(η 1: η 2: η 2-PhPC₄H₃Me)] and
385 [Ru₂(CO)₄(PhPC₄H₃Me)₂], *Inorg. Chim. Acta* 404(0) (2013) 77-81.
- 386 [30] Y. Otero, D. Peña, Y. De Sanctis, A. Arce, E. Ocando-Mavarez, R. Machado, T. Gonzalez, Reactivity of triosmium
387 clusters with 3,4-dimethyl-1-phenylphosphole and cyanoethyl-di-tert-butylphosphine ligands: X-ray crystal structures of
388 [Os₃(CO)₉(μ -OH)(μ -H)(η 1-PhPC₄H₂Me₂)] and [Os₃(CO)₁₁(η 1- t Bu₂PC₂H₄CN)], *Transition Met. Chem.* 39(2)
389 (2014) 239-246.
- 390 [31] Y. Otero, D. Peña, A. Arce, M. Hissler, R. Réau, Y. De Sanctis, E. Ocando-Mavárez, R. Machado, T. González,
391 Fluxional behaviour of phosphole and phosphine ligands on triosmium clusters, *J. Organomet. Chem.* 799–800 (2015)
392 45-53.
- 393 [32] C. Fave, M. Hissler, T. Kárpáti, J. Rault-Berthelot, V. Deborde, L. Toupet, L. Nyulászi, R. Réau, Connecting π -
394 Chromophores by σ -P–P Bonds: New Type of Assemblies Exhibiting σ - π -Conjugation, *J. Am. Chem. Soc.* 126(19)
395 (2004) 6058-6063.
- 396 [33] A. Decken, F. Bottomley, B.E. Wilkins, E.D. Gill, Organometallic Complexes of Benzannelated Phospholyls:
397 Synthesis and Characterization of Benzophospholyl and the First iso-Benzophospholyl Metal Complexes,
398 *Organometallics* 23(15) (2004) 3683-3693.
- 399 [34] R.F.W. Bader, *Atoms in molecules—a quantum theory*, Clarendon Press, Oxford, *Atoms in molecules—a quantum*
400 *theory*, Clarendon Press, Oxford (1990).
- 401 [35] M.I. Bruce, P.J. Low, Expedient synthesis of Re₃(μ -H)₃(CO)₁₁(NCMe), *J. Organomet. Chem.* 519(1) (1996)
402 221-222.

- 403 [36] A. Inc., DMol3 is available as part of Material Studio San Diego, USA, DMol3 is available as part of Material
404 Studio San Diego, USA (2010).
- 405 [37] B. Delley, An all-electron numerical method for solving the local density functional for polyatomic molecules, The
406 Journal of Chemical Physics 92(1) (1990) 508-517.
- 407 [38] S. Aime, R. Gobetto, E. Valls, NMR characterization of four new isomers of H(μ -H)Os₃(CO)₁₀(phosphine),
408 Inorg. Chim. Acta 275–276(0) (1998) 521-527.
- 409 [39] J.P. Perdew, Y. Wang, Accurate and simple analytic representation of the electron-gas correlation energy, Physical
410 Review B 45(23) (1992) 13244-13249.
- 411 [40] B. Delley, From molecules to solids with the DMol3 approach, The Journal of Chemical Physics 113(18) (2000)
412 7756-7764.
- 413 [41] D. Vega, D. Almeida, J. Comput. Methods Sci. Eng., J. Comput. Methods Sci. Eng. 14, 1-3 (2014) 131-136.
414

(η^5 -phospholyl)rhenium complex is obtained from the Re–Re and P–P bonds cleavage.

A phospholyl unit inserted into a M–M bond represents the 2nd example.

A new tetranuclear cluster with two μ -phosphides units is obtained.

ACCEPTED MANUSCRIPT

A ruthenium tetranuclear cluster with two π -conjugated phospholyl units coordinated as μ -phosphide and a (η^5 -phospholyl)rhenium complex are obtained from M-M and P-P bonds cleavage.

ACCEPTED MANUSCRIPT